



UNIVERSITY OF LEEDS

This is a repository copy of *Frequency-selectable dual-band wilkinson divider/combiner*.

White Rose Research Online URL for this paper:

<http://eprints.whiterose.ac.uk/82382/>

Version: Accepted Version

---

**Article:**

Chongcheawchamnan, M, Julrat, S, Shafique, MF et al. (1 more author) (2013)  
Frequency-selectable dual-band wilkinson divider/combiner. *IET Microwaves, Antennas and Propagation*, 7 (10). 836 - 842. ISSN 1751-8725

<https://doi.org/10.1049/iet-map.2013.0113>

---

**Reuse**

Unless indicated otherwise, fulltext items are protected by copyright with all rights reserved. The copyright exception in section 29 of the Copyright, Designs and Patents Act 1988 allows the making of a single copy solely for the purpose of non-commercial research or private study within the limits of fair dealing. The publisher or other rights-holder may allow further reproduction and re-use of this version - refer to the White Rose Research Online record for this item. Where records identify the publisher as the copyright holder, users can verify any specific terms of use on the publisher's website.

**Takedown**

If you consider content in White Rose Research Online to be in breach of UK law, please notify us by emailing [eprints@whiterose.ac.uk](mailto:eprints@whiterose.ac.uk) including the URL of the record and the reason for the withdrawal request.



[eprints@whiterose.ac.uk](mailto:eprints@whiterose.ac.uk)  
<https://eprints.whiterose.ac.uk/>

# **Frequency-Selectable Dual-Band Wilkinson Divider/Combiner**

**M. Chongcheawchamnan and S. Julrat**

Computer Engineering Department

Prince of Songkla University

Songkhla, Thailand

**M. Farhan Shafique**

Center for Advanced Study in Telecommunication

COMSATS Institute of Information Technology

Islamabad, Pakistan

**I. D. Robertson**

Institute of Microwaves and Photonics

University of Leeds, UK

\*Corresponding author: Mitchai Chongcheawchamnan (mitchai@coe.psu.ac.th).

# Frequency-Selectable Dual-Band Wilkinson Divider/Combiner

A technique for realizing a compact frequency-selectable dual-band Wilkinson divider/combiner is presented in this paper. To provide a frequency-selection function, the band-pass transmission-line transformer in a dual-band device is replaced with a tuneable band-reject transmission-line transformer. To realize this tuneable device, a variable capacitively-loaded spur-line filter is proposed for its compact size. The theory based on an ideal transmission-line circuit is developed to provide a design procedure. The proposed circuits are demonstrated with simulated and measured results of a Wilkinson divider/combiner fabricated on FR4 substrate.

**Keywords:** Wilkinson power divider; dual-band power divider; passive circuits; microwave integrated circuits.

## 1. INTRODUCTION

The Wilkinson power divider/combiner is among the most commonly used passive components in microwave and millimetre-wave circuits and systems [1]-[2]. The conventional design for this component uses quarter-wave lines that operate at a single frequency. With ever increasing demand for multi-band and multifunction mobile/handheld devices, several multiband design techniques have been proposed [3]-[9]. Most previous research works proposed new circuit topologies that are able to operate in several bands simultaneously while their circuit sizes are kept small. However, there is a need to design a multi-band communication system operating in non-concurrent mode, for example in a phased array receiver, a low-noise balanced amplifier, or a satellite transceiver, to name a few.

Phased-array receiver systems have been long applied in satellite and military communications due to the excellent sensitivity performance [10-13]. There is a lot of interest from researchers in applying phased arrays to commercial wireless communication application such as in wireless local area networks and cellular mobile systems. In radar, a phased-array can track multiple targets. In these applications, a multi-band or a wideband phased-array receiver is needed. A frequency-selectable multi-band power splitter/combiner is a valuable component for the frontend of such systems. The Wilkinson power divider/combiner is a good design choice due to its simple design and implementation. Therefore, in this paper we demonstrate a simple design for a frequency-selectable dual-band power divider/combiner. The proposed concept can be extended to design a frequency-selectable multi-band power divider/combiner as well.

One way to realise a frequency selectable dual-band Wilkinson divider/combiner is simply to connect two circuits in parallel which operate in the two desired bands. The operating band can be selected by using electronic, mechanical, or optical switching techniques. Unfortunately this simple approach leads to a bulky design. On the other hand, most of the previously proposed dual-band Wilkinson circuits are not appropriate because they lack any frequency selection mechanism.

In this paper, we present a simple concept to design a frequency-selectable dual-band Wilkinson divider/combiner. Starting with a dual-band circuit, a frequency-selectable function is achieved by embedding a band-reject transmission-line transformer (TLT) which has a tuning mechanism. Such a TLT can suppress an unwanted signal in the reject band while allowing the wanted signal through in another band. Recently, a capacitively-loaded spur-line section was proposed for a tuneable band-reject filter [14]. This circuit is compact and can be applied as a tuneable band-

reject TLT. To illustrate this, we apply the frequency-selectable TLT concept to two previously proposed dual-band circuits [7]-[8]. This results in a frequency-selectable dual-band Wilkinson divider/combiner. This design is chosen due to its compact size and simple implementation. It should be noted that the proposed concept can also be applied to other circuits.

The proposed concept, as well as the variable capacitively-loaded spur-line filter will be described in Section 2. The design and implementation of the proposed Wilkinson divider/combiner are presented in Section 3, while the measured results are given in Section 4. Finally, the paper will be concluded in Section 5.

## **2. FREQUENCY-SELECTABLE DUAL-BAND TRANSMISSION-LINE TRANSFORMER**

A single-band Wilkinson divider/combiner can be realized with a TLT. The main concept proposed here to realize a dual-band component for these two circuits is to replace a standard TLT with a dual-band TLT [3]-[4]. This is also applicable for several multi-band designs [5]. In a similar way, designing a frequency-selectable dual-band Wilkinson divider/combiner can be achieved by adding a frequency selectable mechanism to a dual-band TLT in those conventional dual-band designs.

Several network topologies for a dual-band transformer have been proposed. The basic component is a transmission line. A dual-band TLT may be simply designed by cascading several transmission line circuits as shown in Figure 1. A two-section TLT is one of the dual-band transformer design examples which can be achieved by cascading two transmission line sections. Cascading three sections can be done in the form of either a T- or  $\Pi$ -network. For such a case, a one-port network topology realized with either a short or open circuit transmission line is needed. It should be noted that a dual-band transformer formed with a symmetrical T- or  $\Pi$ -network is preferable for

realizing a symmetrical microwave circuit. As it is more generally applicable than the two-section TLT, we therefore develop a frequency-selectable dual-band transformer based on a T- or  $\Pi$ -network topology.

By adding a mechanism to control the passband in the T- or  $\Pi$ -network shown in Figure 1, a tuneable band reject function is given to the transmission line in the three-section network. This may be achieved by either cascading a tuneable band reject filter (BRF) to the network or replacing the transmission line with a tuneable BRF. Either way, the size of the new circuit should be negligibly increased as compared with the original size. The approach to cascade a BRF with the network shown in Figure 1 is not of interest since it unavoidably increases the circuit size. We therefore choose the second approach and apply it to the three-section network.

A variable capacitively-loaded spur-line filter shown in Figure 2a) is selected as a tuneable BRF in this paper due to its compact size [14]. It is composed of a spur-line filter with a variable capacitor connected across the ends of the coupled lines. This tuneable spur-line filter is characterized by its characteristic impedance and electrical length. Here, we will only focus on a spur line design based on symmetrical coupled lines. We assume that the coupled lines are lossless, hence the ideal transmission-line model can be applied when the tuneable spur line is analyzed. The even- and odd-mode characteristic admittances of the coupled lines in Figure 2(a) are denoted by  $Y_{0e}$  and  $Y_{0o}$ . The electrical length defined at the first operating frequency  $f_1$  is  $\theta$ . The coupling coefficient of the coupled lines determines the bandwidth for each stopband and also the response of the circuit. Tight coupling is needed if a narrow stopband is desired. However, the fabrication limitations have to be carefully considered in practice. The variable capacitor  $C_i$  ( $i = 1,2$ ) provides a mechanism to tune a stopband frequency at

$f_i$ . With a system admittance  $Y_0$  defined at spur-line ports a and b, the scattering parameters at frequency  $f$  of this tuneable spur line filter are [14]:

$$s_{aa}(f, C_i) = \frac{1}{\Delta(f, C_i)} \left[ Y_0^2 \left\{ (Y_{0e} + Y_{0o}) \cot\left(\theta \frac{f}{f_1}\right) - 4\pi f C_i \right\} + 4Y_{0e}^2 \left\{ 4\pi f C_i - Y_{0o} \cot\left(\theta \frac{f}{f_1}\right) \right\} - j2Y_0 Y_{0e}^2 \right] \quad (1a),$$

$$s_{ab}(f, C_i) = s_{ba}(f, C_i) = \frac{j4Y_0 Y_{0e} \csc\left(\theta \frac{f}{f_1}\right) \left[ 4\pi f C_i - Y_{0o} \cot\left(\theta \frac{f}{f_1}\right) \right]}{\Delta(f, C_i)} \quad (1b),$$

$$s_{bb}(f, C_i) = \frac{1}{\Delta(f, C_i)} \left[ Y_0^2 \left\{ (Y_{0e} + Y_{0o}) \cot\left(\theta \frac{f}{f_1}\right) - 4\pi f C_i \right\} + 4Y_{0e}^2 \left\{ 4\pi f C_i - Y_{0o} \cot\left(\theta \frac{f}{f_1}\right) \right\} + j2Y_0 Y_{0e}^2 \right] \quad (1c),$$

where

$$\begin{aligned} \Delta(f, C_i) = & Y_0^2 \left\{ (Y_{0e} + Y_{0o}) \cot\left(\theta \frac{f}{f_1}\right) - 4\pi f C_i \right\} + 4Y_{0e}^2 \left\{ Y_{0o} \cot\left(\theta \frac{f}{f_1}\right) - 4\pi f C_i \right\} \\ & + j2Y_0 Y_{0e} \left\{ Y_{0e} + 8\pi f C_i \cot\left(\theta \frac{f}{f_1}\right) - 2Y_{0o} \left[ \cot\left(\theta \frac{f}{f_1}\right) \right]^2 \right\} \end{aligned} \quad (1d).$$

By inspecting only (1b), one can find that the frequency stopband at  $f_i$  will be obtained if  $C_i$  is tuned to:

$$C_i = \frac{Y_{0o} \cot\left(\frac{f_i \theta}{f_1}\right)}{4\pi f_i} \quad (2).$$

Substituting (2) into (1a)-(1d) and simplifying further, the frequency responses of the tuneable spur line at  $f_i$  are:

$$s_{aa}(f_i) = \frac{Y_0 \cot\left(\frac{\theta f_i}{f_1}\right) - j2Y_{0e}}{Y_0 \cot\left(\frac{\theta f_i}{f_1}\right) + j2Y_{0e}} \quad (3a),$$

$$s_{ab}(f_i) = s_{ba}(f_i) = 0 \quad (3b),$$

$$s_{bb}(f_i) = 1 \quad (3c).$$

As is clearly shown in (3b), the spur-line filter provides a stopband at  $f_i$ . The magnitudes of input and output reflection coefficients are equal to one with very tightly coupled lines. The effect of coupling coefficient on the circuit performances is very critical, especially with a very narrowband circuit.

Based on the T- and  $\Pi$ -networks shown in Figure 1 as well as the tuneable spur-line filter shown in Figure 2a), Figure 2b) shows two proposed networks for realizing a frequency-selectable dual-band TLT. From Figure 2b), if the design parameters of the tuneable spur-line filter match with those of the transmission line which is to be replaced, a frequency-selectable dual-band TLT will be obtained. The tuneable spur line replaces a series or shunt transmission-line section in the  $\Pi$ - or T-network topologies, respectively. Although bias circuitry is needed for the tuning mechanism, the circuit size of the proposed TLT can be designed to be almost the same as that of the conventional one.

Application of the proposed technique to the dual-band Wilkinson divider/combiner is shown in Figure 3. As shown, the proposed spur-line filter replaces a transmission-line circuit. A varactor diode ( $D_1$ ) is used for a variable capacitor in the tuneable filter. It should be noted that other tuning devices, for example mechanical or optically-controlled components could also be used. A simple resistive bias circuit is applicable as the varactor diode is reverse biased and consumes very small current. The control voltage ( $V_{CTRL}$ ) is applied through the reversed bias resistor ( $R_{bias}$ ). The capacitor ( $C_a$ ) is used to block the DC reversed bias current and prevent a short circuit

occurring at the coupled lines. Since the electrical length of the tuneable spur line is equal to that of the replaced transmission-line section, the overall size of the proposed frequency-selectable dual-band Wilkinson divider/combiner is similar to the size of the original designs which were reported in [7] and [8].

The design procedure for these two proposed circuits can be summarized in Figure 4. Defining system impedance ( $Z_0$ ) and two desired frequencies ( $f_1, f_2$ ), a dual-band component is synthesized from the procedure presented in [7]-[8]. With the proposed designs depicted in Figure 3, a number of transmission lines are replaced with the tuneable coupled lines. A tuning capacitance range for the tuned coupled lines is calculated from (2), hence an appropriate varactor diode will be selected. Next, the reversed bias circuitry needed for the proposed design will be synthesized. With all electrical synthesized parameters, all circuit dimensions will be calculated. An optimization process is needed during the design and layout process.

### **3. DESIGN AND IMPLEMENTATION**

The validity of the proposed technique is demonstrated by designing a frequency-selectable dual-band Wilkinson divider/combiner operating at 1 and 2 GHz on a FR4 substrate. The target return loss and isolation performances of the design for the operating bands are -15 dB while  $S_{21}$  and  $S_{31}$  at the off-band are expected to be lower than -10 dB. The thickness of a substrate is 1.5 mm and the dielectric constant is 4.5. Having followed the design procedure presented in Figure 4, the Wilkinson divider/combiner is designed in microstrip form. The physical parameters after optimizing the design performances are summarized in Table I. The final size of the Wilkinson circuit is  $24.75\text{cm}^2$ .

The coupling gaps for the frequency-selectable dual-band Wilkinson divider/combiner were selected as 0.5 mm, since these gaps can be readily implemented

with the in-house fabrication process. Variable capacitors in the circuits are implemented with a BB857 varactor diode in the surface mount device (SMD) package. The capacitor range of this diode is 0.5-6.6 pF when a reverse bias range of 0 to 30 V is applied. A resistor of 56 k $\Omega$  is selected for biasing this diode. The isolation resistor,  $R_{ISO1}$ , in the Wilkinson divider/combiner is selected as 100 $\Omega$ . A surface mount technology (SMT) capacitor of 40 pF was selected for the DC blocking capacitor.

The circuit was laid out using the Agilent Technologies Momentum<sup>TM</sup> software. A symmetrical layout was required to preserve the symmetrical property of the circuit response. The diode model presented in [15]-[16] was included in the simulation. The values of parasitic components for the SMD package are illustrated in Figure 5. The open transmission lines in the Wilkinson divider/combiner were converted to curved lines to minimize the circuit size,  $t$ . The ends of each transmission line pair at port 2 and 3 are tapered such that the gap between -port 2 and 3 fit with the size of SMT isolation resistor (model 0405). This leads to good matching and isolation at port 2 and 3 for the Wilkinson design at both frequencies.

The simulated scattering parameters of the design using Momentum<sup>TM</sup> are shown in Figure 6. Figure 6 a) and b) demonstrate the performances of the Wilkinson divider/combiner. The results show good matching at all ports for both bands. The performance of the Wilkinson circuit is not very sensitive to coupling coefficient since the operating band of the Wilkinson circuit is generally broad.

#### **4. MEASURED RESULT AND DISCUSSIONS**

Photograph of the Wilkinson circuit is shown in Figure 7. The measurements were performed with a vector network analyzer (HP8510C). A short-open-load-thru (SOLT) calibration from 0.05-6 GHz was performed before making measurement. SMA connectors were used to interface the circuits with the network analyzer via coaxial

cables. The bias voltage was applied from a power supply (GPR-3510HD). By terminating with a  $50 \Omega$  standard SMA load, each two-port scattering parameter set was measured. All data sets were collected and post processed using the Agilent Technologies Advanced Design System™.

Figure 8 a) and b) show the measured  $S_{11}$ ,  $S_{21}$ ,  $S_{31}$  and  $S_{23}$  of the Wilkinson circuit when the reverse bias is applied at 0 and 25 V, respectively. Excellent amplitude balance between port P2 and P3 is obtained for the two reversed bias conditions. When 0 V is applied, the operating frequency shifts from the designed 2 GHz to 2.2 GHz as shown in Figure 8a). On the other hand, the operating frequency shifts from the designed 1 GHz to 1.2 GHz when 25 V is applied as shown in Figure 8b). This frequency shift is expected from the limitation of our fabrication tolerance and the parasitics of SMD components. From Table 2, the matching and isolation performances are better than -18 dB in both operating bands.  $S_{21}$  and  $S_{31}$  are around -3.8 dB in both operating bands. We believe that the increased loss mainly results from the parasitic resistance from the diode and the DC blocking capacitor used in our design. The straightforward method to obtain low insertion loss in these circuits is to choose other low loss tuning techniques, for example an optical or ferromagnetic tuning technique.

Figure 9 a) and b) shows the phase balance performance of the Wilkinson circuit for two reversed bias voltages, 0 and 25 V, respectively. Excellent phase balance occurs in both bands for each reversed bias condition. This is comes from the symmetrical layout in our design.

## **5. CONCLUSION**

A frequency-selectable Wilkinson divider based on the proposed frequency-selectable dual-band transmission-line transformer has been demonstrated. The mechanism for tuning the frequency of the transmission-line transformer is a capacitively-loaded spur-

line filter using a varactor diode. It has been shown that this frequency-selectable Wilkinson divider provides a compact design and is hence suited for low-cost solutions. Compared with the prototype dual-band structure, no extra area is needed for the proposed technique. We also present the design procedure for the proposed circuits. Experimental results show the feasibility of the technique. Parasitic resistance from the varactor diode and DC blocking capacitor should be carefully taken into account during the design. To obtain better performance for the proposed design, other low loss tuning techniques are recommended. We believe that the proposed components suits for a number of applications including phased-array receivers.

## **ACKNOWLEDGEMENT**

This research is financially supported by Telecommunications Research & Industrial Development Institute (TRIDI) under grant number TARG 2553/004. Ian D. Robertson would like to acknowledge the support of EPSRC (3D Microwave & Millimetre-Wave System-on-Substrate using Sacrificial Layers for Printed RF MEMS Components).

## **REFERENCES**

1. Chang, K., Encyclopedia of RF and Microwave Engineering, Wiley-Interscience, 2005.
2. Robertson, I. D. and S. Lucyszyn, RFIC and MMICs design, IEE, 2002.
3. Srisathit, S., S. Virunphun, K. Bandudej, M. Chongcheawchamnan, and A. Worapishet, "A dual-band 3-dB three-port power divider based on a two-section transmission line transformer," in IEEE MTT-S Int. Microwave Symp. Dig., Vol. 1, 35–38, 2003.

4. Srisathit, S., M. Chongcheawchamnan, A. Worapishet, "Design and realisation of a dual-band 3-dB power divider based on a two-section transmission-line topology," *Electronics Letters*, Vol. 29, No. 9, 723-724, 2003.
5. Chongcheawchamnan, M., S. Patisang, M. Krairiksh, and I. Robertson, "Tri-band Wilkinson power divider using a three-section transmission-line transformer," *IEEE Microw. Wireless Compon. Lett.*, Vol. 16, No.8, 452–454, 2006.
6. Qaroot, A. M. and N. I. Dib, "General design of n-way multi-frequency unequal split Wilkinson power divider using transmission line transformers," *Progress In Electromagnetics Research C*, Vol. 14, 115-129, 2010.
7. Wu, L., Z. Sun, H. Yilmaz, and M. Berroth, "A dual-frequency Wilkinson power divider", *IEEE Trans. on Microwave Theory and Techniques*, Vol. 54, No.1, 278-284, 2006.
8. Cheng, K.-K. M., and F.-L. Wong, "A new Wilkinson power divider design for dual-band applications," *IEEE Microw. Wireless Compon. Lett.*, Vol. 17, No.9, 664–666, 2007.
9. Power divider and power combiner using dual-band composite right/left handed transmission line, United States Patent, US 2010/0026416 A1.
10. Jeon S. et al., "A scalable 6-to-18 GHz concurrent dual-band quad-beam phased-array receiver in CMOS", *IEEE Journal of Solid-State Circuits*, Vol. 43, No.12, 2660-2673, 2008.
11. Katajamaki, T. Radionet, "A compact dual-band phased array antenna for outdoor WLAN", *IEEE Vehicular Technology Conference*, Vol.1, 59-63, 2004.
12. Choi, H. J. and T. Itoh, "Dual-band composite right/left-handed (CRLH) phased-array antenna," *IEEE Antenna and Wireless Propagation Letters*, Vol. 11, 732-735, 2012.

13. Kim, J., J. Jeong and S. Jeon, "Improvement of noise performance in phased-array receivers," ETRI Journal, Vol. 33, No.2, 176-183, 2011.
14. Chongcheawchamnan, M., M. F. Shafique and I. D. Robertson, "Miniaturization and electronic tuning techniques for microstrip spuline filters," IET Microws., Antennas, and Prop., Vol. 5, No.1, 1-9, 2011.
15. Infineon Technologies AG: BB857 Data Sheet and BB857 Simulation Data, <http://www.infineon.com>, January 2009.
16. Vokac, M., "Phase shifter based on varactor-loaded transmission line", Master Thesis, Department of Electromagnetic Field, Faculty of Electrical Engineering, Czech technical university, 2009.

## **List of Table**

Table 1. Dimensions (in mm) of the Wilkinson divider/combiner implementing on FR4

Table 2. Simulated and measured S-parameter of the proposed design

Table 1. Dimensions (in mm) of the Wilkinson divider/combiner implementing on FR4

Parameter	Value
Width of transmission line 1	3.8
Length of transmission line 1	12.7
Width of transmission line 2	4
Length of Transmission line 2	25.5
Coupled lines length	8.2
Coupled lines gap	0.5
Coupled lines width	1.6
Open-end transmission line length	55.5
Open-end transmission line width	2

Table 2. Simulated and measured S-parameter of the proposed design

0 V	S11		S12		S22		S13		S33		S23	
f (GHz)	Sim.	Mea.										
0.8	-1.0	-1.0	-17.0	-22.0	-4.0	-3.0	-17.0	-22.0	-4.0	-3.0	-10.0	-15.0
0.9	-4.0	-2.5	-10.0	-12.0	-7.0	-5.0	-10.0	-12.0	-7.0	-5.0	-10.0	-10.0
1.0	-7.3	-7.5	-5.0	-5.0	-14.0	-12.0	-5.0	-5.0	-14.0	-12.0	-12.5	-13.0
1.1	-5.0	-10.0	-7.0	-5.0	-10.0	-17.5	-7.0	-5.0	-10.0	-16.5	-12.0	-15.0
1.2	-3.0	-7.0	-15.0	-9.0	-5.0	-9.0	-15.0	-9.0	-5.0	-10.0	-25.0	-30.0
1.3	-6.0	-8.0	-5.0	-6.0	-14.0	-14.0	-5.0	-6.0	-14.0	-15.5	-12.0	-17.0
1.8	-23.0	-10.0	-3.7	-4.3	-18.0	-15.0	-3.7	-4.3	-17.0	-15.0	-10.0	-7.0
1.9	-18.0	-11.0	-3.7	-4.3	-24.0	-20.0	-3.7	-4.3	-21.0	-20.0	-14.0	-9.0
2	-20.0	-12.0	-3.7	-4.3	-25.0	-22.5	-3.7	-4.3	-22.0	-22.5	-18.0	-13.0
2.1	-13.0	-15.0	-6.0	-4.3	-14.0	-25.0	-6.0	-4.3	-14.0	-25.0	-13.0	-18.0
2.2	-2.0	-15.0	-15.0	-4.3	-10.0	-25.0	-15.0	-4.3	-10.0	-25.0	-12.0	-20.0
2.3	-3.0	-5.0	-15.0	-4.3	-5.0	-12.0	-15.0	-4.3	-6.0	-12.0	-13.0	-12.0
25 V	S11		S12		S22		S13		S33		S23	
f (GHz)	Sim.	Mea.										
0.8	-1.0	-1.0	-19.0	-24.0	-3.8	-3.0	-19.0	-24.0	-3.8	-3.0	-10.5	-15.0
0.9	-3.0	-2.0	-10.0	-12.0	-7.0	-5.0	-10.0	-12.0	-7.0	-5.0	-10.0	-11.0
1.0	-11.0	-10.0	-4.5	-5.0	-15.0	-13.0	-4.5	-5.0	-15.0	-13.0	-15.0	-15.0
1.1	-18.0	-20.0	-3.7	-3.7	-25.0	-25.0	-3.7	-3.7	-25.0	-25.0	-18.0	-23.0
1.2	-19.0	-23.0	-3.7	-3.7	-23.0	-28.0	-3.7	-3.7	-23.0	-28.0	-14.0	-22.0
1.3	-19.5	-18.0	-3.7	-3.7	-14.0	-23.0	-3.7	-3.7	-14.0	-23.0	-9.5	-12.0
1.8	-9.0	-15.0	-4.0	-3.9	-9.8	-11.0	-4.0	-3.9	-8.5	-11.0	-20.0	-13.0
1.9	-7.0	-12.0	-4.8	-4.0	-10.0	13.0	-4.8	-4.0	-9.0	-12.0	-23.0	-20.0
2	-4.0	-7.0	-6.0	-4.5	-11.5	13.0	-6.0	-4.5	-10.5	-12.0	-12.0	-20.0
2.1	-2.2	-3.8	-10.0	-7.0	-9.5	-11.0	-10.0	-7.0	-9.5	-11.0	-8.6	-12.0
2.2	-1.5	-1.5	-20.0	-13.0	-10.0	-8.0	-20.0	-13.0	-10.0	-8.0	-12.0	-8.0
2.3	-2.0	2.2	-20.0	-23.0	-6.5	-7.0	-20.0	-18.0	-7.0	-7.0	-18.0	-9.0

## List of Figures

Figure 1. Dual-band transformer realization with double and triple cascaded networks

Figure 2. a) Variable capacitively-loaded spur line; b) its application to the dual-band TLT

Figure 3. Application of the frequency-selectable dual-band TLT to dual-band Wilkinson divider/combiner

Figure 4. Design flow of the proposed frequency-selectable Wilkinson divider/combiner

Figure 5. Parasitic model of a varactor diode BB857

Figure 6. Simulated scattering parameters of the Wilkinson divider/combiner when applying a reversed bias voltage of a) 0V and b) 25 V

Figure 7. Photograph of the frequency-selectable dual-band Wilkinson divider/combiner

Figure 8. Measured amplitude, input matching and isolation responses of the Wilkinson circuit when the reversed bias is applied at a) 0 and b) 25 V

Figure 9. Phase balance of the Wilkinson circuit when applying the reversed bias voltage, a) 0 and b) 25 V

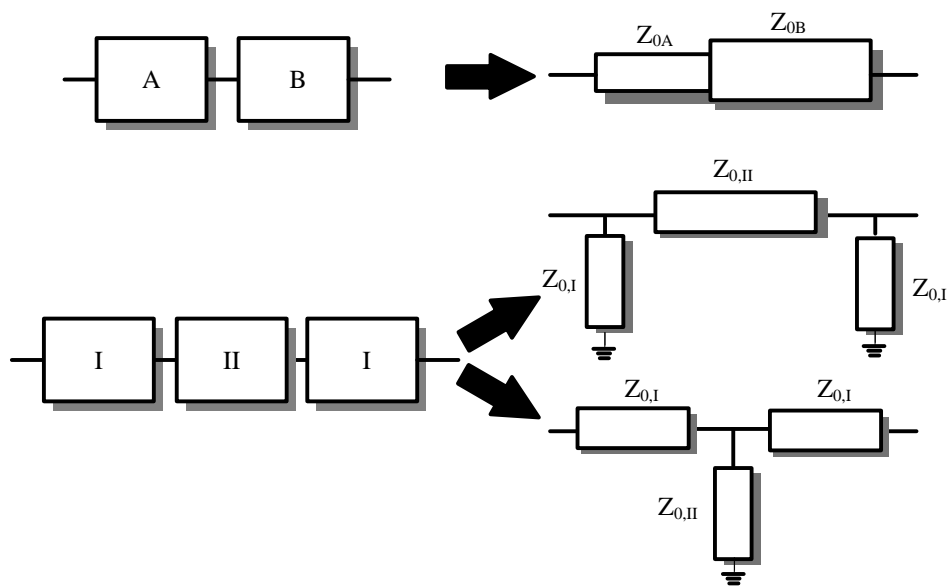
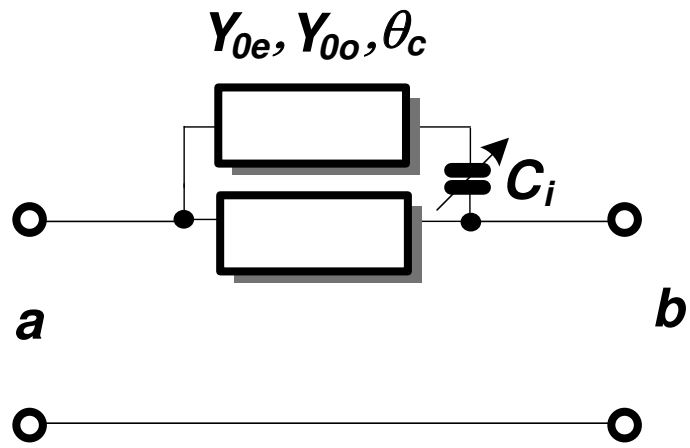
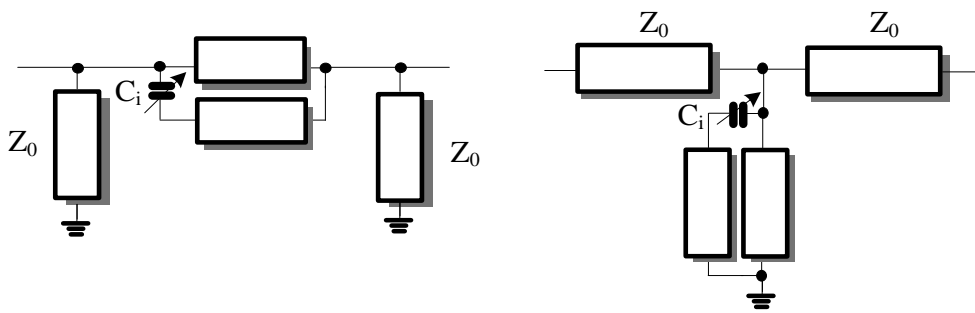


Figure 1 Dual-band transformer realization with double and triple cascaded networks



a)



b)

Figure 2 a) Variable capacitively-loaded spur line; b) its application to the dual-band

TLT

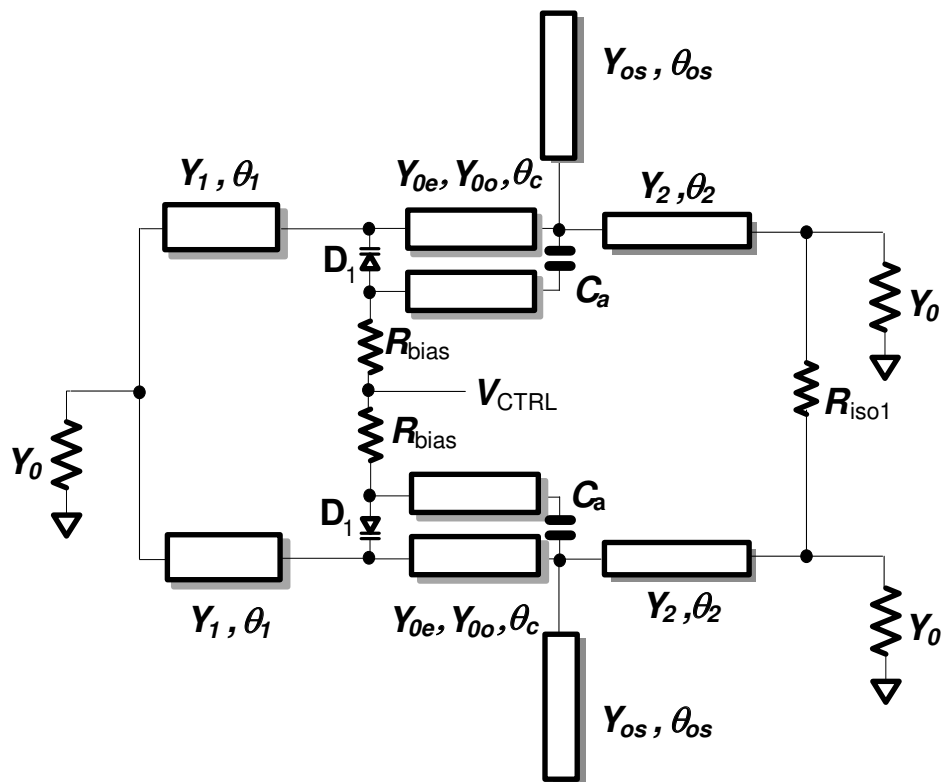


Figure 3 Application of the frequency-selectable dual-band TLT to dual-band Wilkinson divider/combiner

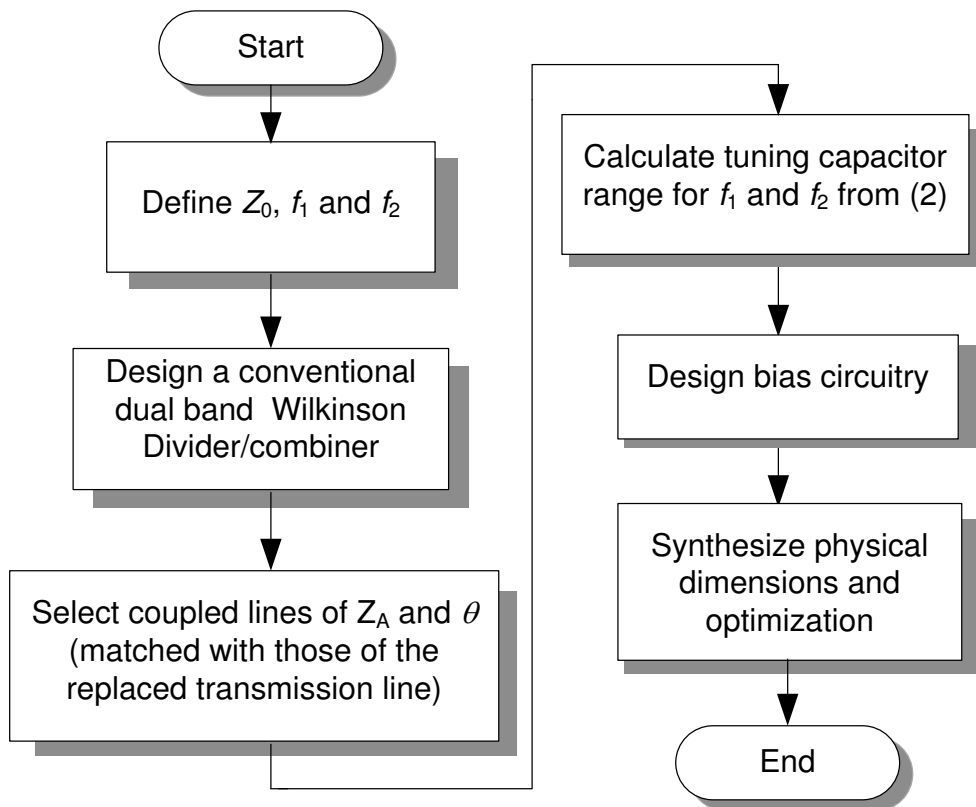


Figure 4 Design flow of the proposed frequency-selectable Wilkinson divider/combiner

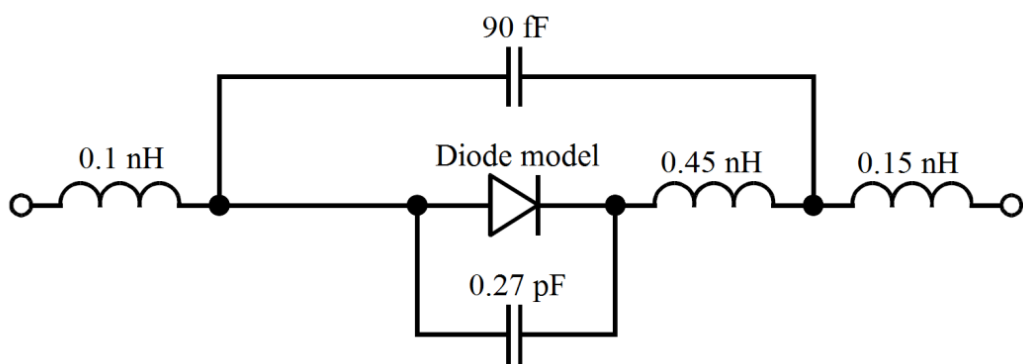
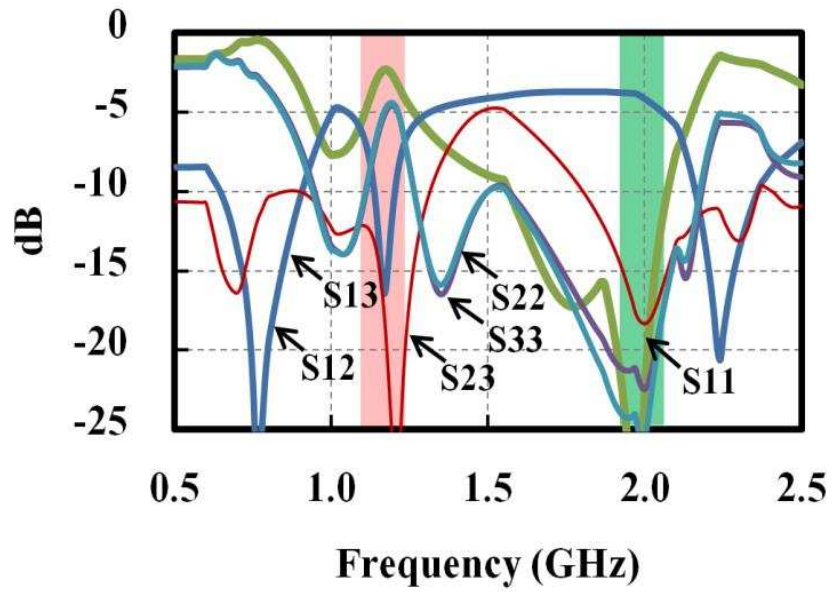
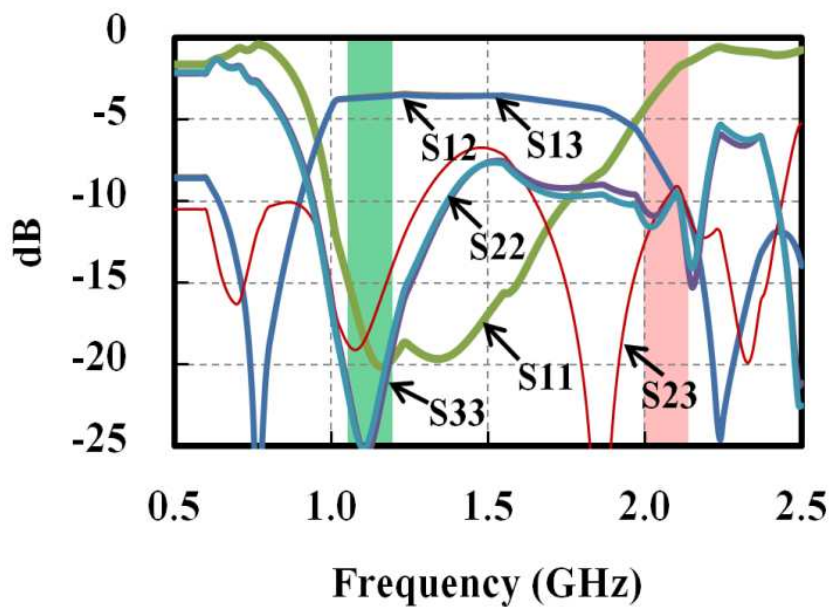


Figure 5 Parasitic model of a varactor diode BB857



a)



b)

Figure 6 Simulated scattering parameters of the Wilkinson divider/combiner when applying a reverse bias voltage of a) 0V and b) 25 V

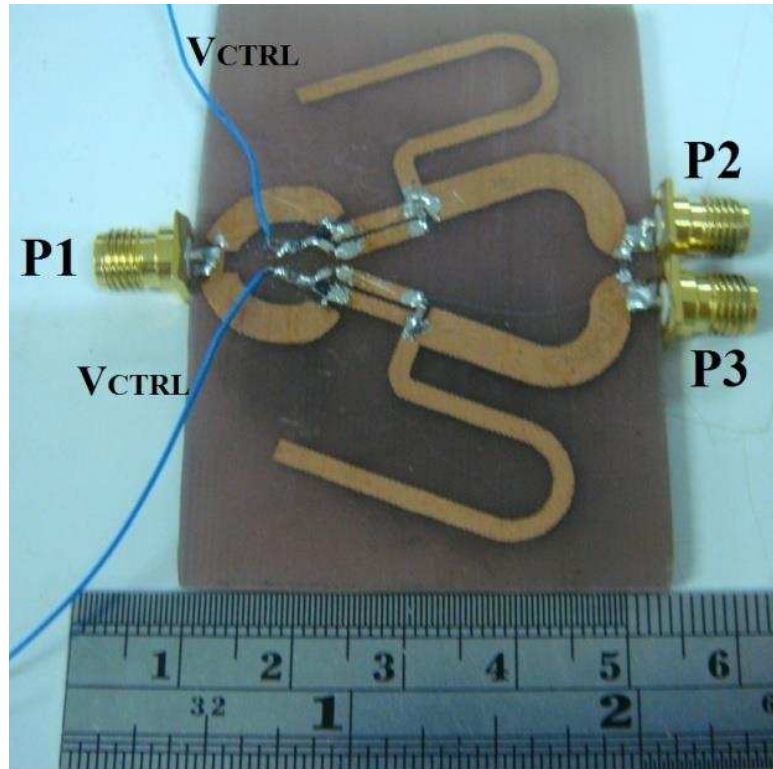
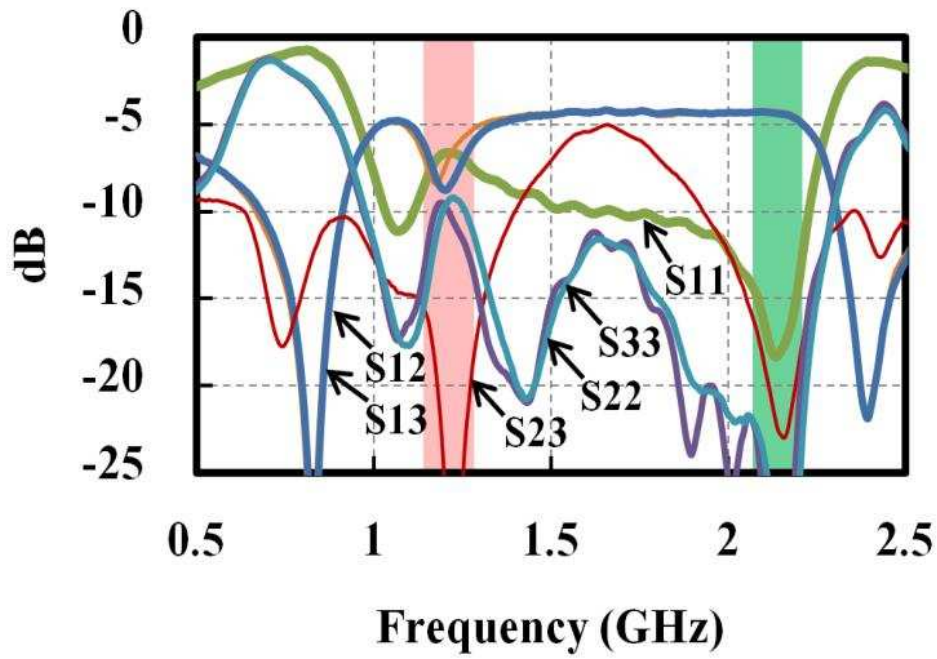
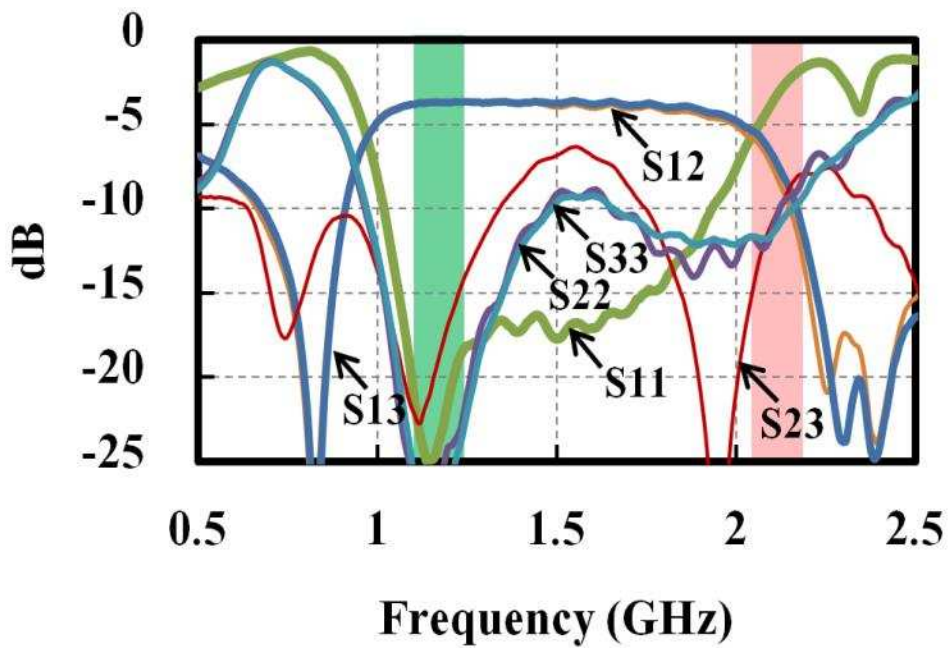


Figure7 Photograph of the frequency-selectable dual-band Wilkinson divider/combiner

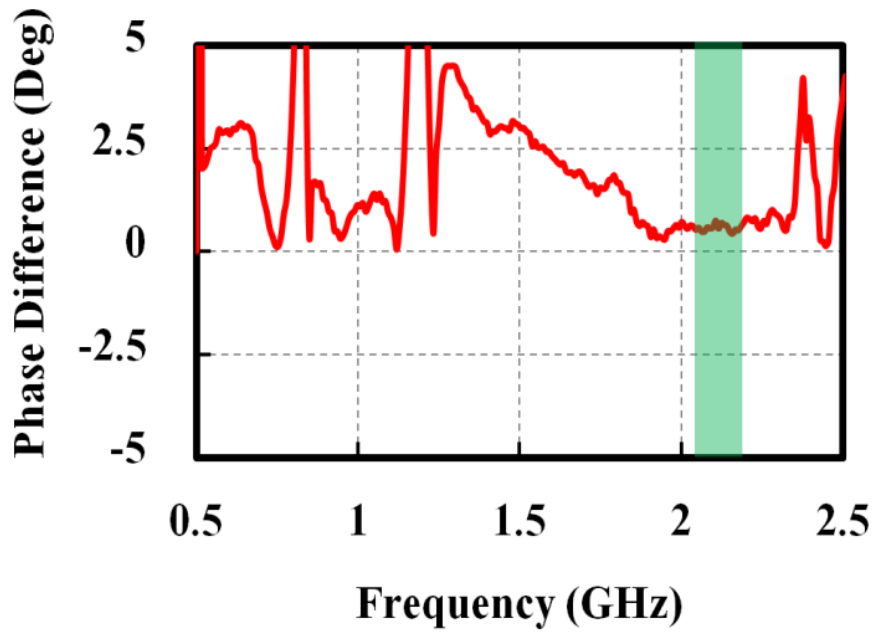


a)

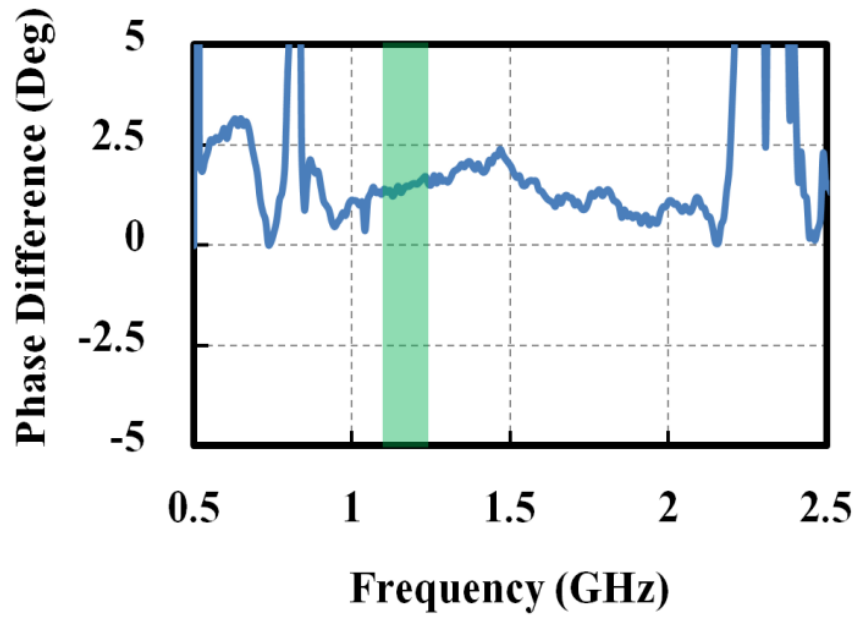


b)

Figure 8. Measured amplitude, input matching and isolation responses of the Wilkinson circuit when the reversed bias is applied at a) 0 and b) 25 V.



a)



b)

Figure9. Phase balance of the Wilkinson circuit when applying the reversed bias voltage, a) 0 and b) 25 V